2015 IEEE 54th Annual Conference on Decision and Control (CDC)
December 15-18, 2015. Osaka, Japan

Decentralized optimal control of inter-area oscillations in bulk power systems

Xiaofan Wu, Florian Dörfler, and Mihailo R. Jovanović

Abstract— **In bulk power systems, spectral analysis of poorly damped modes is commonly used for identifying local and inter-area oscillations. Conventionally, these oscillations are mitigated by carefully tuned decentralized controllers. In this paper, we depart from the modal perspective and employ non-modal tools to analyze and control inter-area oscillations. Our input-output analysis examines power spectral density and variance amplification of stochastically forced systems and offers new insights relative to modal approaches. To improve upon the limitations of conventional wide-area control strategies, we also study the problem of signal selection and optimal design of sparse and block-sparse wide-area controllers. In our approach, we preserve rotational symmetry of the power network by allowing only relative angle measurements in the distributed controllers. We examine performance tradeoffs and robustness of sparse and block-sparse control architectures by studying the NETS-NYPS test system, and show that optimal retuning of fully-decentralized controllers can effectively guard against local and inter-area oscillations.**

Index Terms— **Decentralized control, input-output analysis, inter-area oscillations, power systems, sparsity-promoting optimal control, synchronization, wide-area control.**

I. Introduction

Electromechanical oscillations in power systems are mainly caused by the loss of synchronization among the generators and imbalanced power transfers. In particular, oscillations with low frequencies and poor damping that involves groups of generators swinging against each other, are identified as inter-area oscillations. In recent years, increasing system loads and deployment of renewables in remote areas have significant impact on the dynamical behavior and system stability. Limitations on the existing transmission network would lead to smaller stability margins and even power outage [1].

Conventional study on inter-area oscillations are based on modal analysis of the system dynamics. Modal approaches identify inter-area oscillations from the spatial profile of the eigenvectors and participation factors of the poorly damped modes. In practice, decentralized control gains are carefully tuned to damp inter-area oscillations, using root locus [2], pole placement [3] and optimal control [4] strategies. However, these decentralized control actions can interact in an adverse way and may even destabilize the overall system.

Financial support from ETH Zürich startup grants, the University of Minnesota Informatics Institute Transdisciplinary Faculty Fellowship, and the National Science Foundation under award ECCS-1407958 is gratefully acknowledged.

Xiaofan Wu and Mihailo R. Jovanović are with the Department of Electrical and Computer Engineering, University of Minnesota, Minneapolis, MN 55455. Emails: [wuxxx836,mihailo]@umn.edu. Florian Dörfler is with the Automatic Control Laboratory at ETH Zürich, Switzerland. Email: dorfler@control.ee.ethz.ch.

To improve the performance of existing decentralized control strategy, recent effort aims at designing wide-area controllers that use remote measurements to form local control actions [5]. These wide-area control design approaches range from root locus criteria to robust and optimal control [6], to maximize modal observability [7]. In this paper, we use an input-output analysis to examine power spectral density and variance amplification of the stochastically forced power systems. In previous works [8], [9], a similar approach was employed to quantify performance of consensus and synchronization networks.

Here, we follow the procedures of sparsity-promoting optimal control algorithm [10]–[13], which was successfully employed for wide-area control of power systems [14]–[16]. We formulate the problem following [13], [17] and design linear state feedback controllers that simultaneously optimizes a quadratic optimal control criterion and induces a sparse control architecture. Our approach departs from recent results [14]–[16] at two levels: (i) we preserve rotational symmetry of the original power network by allowing only relative angle measurements in the distributed controller and (ii) we allow identification and optimal feedback gain design of block-sparse control architectures.

We illustrate our developments by testing our control strategy on the NETS-NYPS test system [18], [19]. We show how different sparsity-promoting penalty functions can be used to achieve a desired balance between closed-loop $\mathcal{H}_2$ performance and sparsity of the communication network. The addition of particular remote communication links and careful retuned local control gains are shown to be effective for improving system performance. For the NETS-NYPS test system, the numerical results indicate that properly retuned and *fully-decentralized* controllers can show comparable performance to the optimal centralized controllers.

This paper summarizes the key developments of our recent journal submission [20] and it is organized as follows. In Section II, we briefly introduce the model, discuss causes of inter-area oscillations, and provide background on input-output analysis of power systems. In Section III, we formulate sparse and block-sparse optimal wide-area control problems under the relative angle measurement restriction. In Section IV, we test our sparse controllers on the NETS-NYPS test system and compare performance of open- and closed-loop systems. Finally, Section V concludes the paper.

II. Background on power system oscillations

A. Modeling and control preliminaries

A power network is described by a set of nonlinear differential-algebraic equations. By linearizing around a sta-

tionary operating point and eliminating the algebraic equations, a state-space model is of the form

$$\dot{x} \;=\; A\,x \;+\; B_1\,d \;+\; B_2\,u. \tag{1}$$

Here, $x(t) \in \mathbb{R}^n$ is the state, $u(t) \in \mathbb{R}^m$ is the excitation control input, and $d(t) \in \mathbb{R}^p$ is the stochastic disturbance. For example, the choice $B_1 = B_2$ can be used to account for the impact of communication noise from the input channels [15].

The dominant electro-mechanical dynamics of a power system are well captured by the linearized *swing equations* [21],

$$M_i\,\ddot{\theta}_i \;+\; D_i\,\dot{\theta}_i \;+\; \sum\nolimits_j L_{ij}\,(\theta_i \;-\; \theta_j) \;=\; 0.$$

Here, θ_i and $\dot{\theta}_i$ are the rotor angle and frequency of generator i, M_i and D_i are the generator inertia and damping coefficients, and L_{ij} is the (i,j) element of the network susceptance matrix. Swing equations nicely illustrate the causes of inter-area oscillations, which originate from sparse links between densely connected groups of generators [22].

Under a linear state-feedback $u = -Kx$, the closed-loop system takes the form

$$\begin{aligned} \dot{x} \;&=\; (A \;-\; B_2K)\,x \;+\; B_1\,d \\ z \;&=\; \left[\begin{array}{c} z_1 \\ z_2 \end{array}\right] \;=\; \left[\begin{array}{c} Q^{1/2} \\ -R^{1/2}\,K \end{array}\right] x \end{aligned} \tag{2}$$

where z is a performance output with state and control weights Q and R. We choose R to be the identity matrix and a state objective that quantifies a desired potential energy and the kinetic energy stored in the electro-mechanical dynamics,

$$x^TQ\,x \;=\; \theta^TQ_\theta\,\theta \;+\; \frac{1}{2}\,\dot{\theta}^TM\,\dot{\theta}.$$

Here, $M = \mathrm{diag}\,(M_i)$ is the inertia matrix and Q_θ penalizes deviation of angles from their average $\bar{\theta}(t) := (1/N)\,\mathbb{1}^T\theta(t)$,

$$Q_\theta \;=\; I \;-\; (1/N)\,\mathbb{1}\mathbb{1}^T \tag{3}$$

where N is the number of generators and $\mathbb{1}$ is the vector of all ones. In a power system without a slack bus, the generator rotor angles are only defined in a relative frame of reference, as can be observed in the property of the Laplacian matrix L in the swing equations. Thus, they can be rotated by a uniform amount without changing the fundamental dynamics (1). We preserve rotational symmetry and study problems in which only differences between the components of the vector $\theta(t) \in \mathbb{R}^N$ enter into (2). As a result of rotational symmetry, both open-loop A-matrix and performance weight Q_θ have an eigenvalue at zero which characterizes the mean of rotor angles.

By expressing the state vector as $x(t) := \left[\begin{array}{cc} \theta(t)^T & r(t)^T \end{array}\right]^T$, where $r(t) \in \mathbb{R}^{n-N}$ represents the rotor frequencies and additional states that account for fast electrical dynamics, we arrive at the structural constraints on the matrices in (2),

$$A\left[\begin{array}{c} \mathbb{1} \\ 0 \end{array}\right] \;=\; 0, \quad Q_\theta\,\mathbb{1} \;=\; 0, \quad K\left[\begin{array}{c} \mathbb{1} \\ 0 \end{array}\right] \;=\; 0.$$

To eliminate the average-mode $\bar{\theta}$ from (2) we introduce the following coordinate transformation [13],

$$x \;=\; \left[\begin{array}{c} \theta \\ r \end{array}\right] \;=\; \underbrace{\left[\begin{array}{cc} U & 0 \\ 0 & I \end{array}\right]}_{T}\xi \;+\; \left[\begin{array}{c} \mathbb{1} \\ 0 \end{array}\right]\bar{\theta} \tag{4}$$

where the columns of the matrix $U \in \mathbb{R}^{N\times(N-1)}$ form an orthonormal basis that is orthogonal to span $(\mathbb{1})$. For example, these columns can be obtained from the $(N-1)$ eigenvectors of the matrix Q_θ in (3) that correspond to the non-zero eigenvalues. In the new coordinates, $\xi(t) = T^Tx(t) \in \mathbb{R}^{n-1}$, the closed-loop system takes the form

$$\begin{aligned} \dot{\xi} \;&=\; (\bar{A} \;-\; \bar{B}_2F)\,\xi \;+\; \bar{B}_1\,d \\ z \;&=\; \left[\begin{array}{c} z_1 \\ z_2 \end{array}\right] \;=\; \left[\begin{array}{c} \bar{Q}^{1/2} \\ -\bar{R}^{1/2}\,F \end{array}\right]\xi \end{aligned} \tag{5}$$

where

$$\bar{A} \;:=\; T^TAT, \quad \bar{B}_i \;:=\; T^TB_i, \quad \bar{Q}^{1/2} \;:=\; Q^{1/2}\,T.$$

The feedback matrices K and F (in the original x and new ξ coordinates, respectively) are related by

$$F \;=\; K\,T \quad\Leftrightarrow\quad K \;=\; F\,T^T.$$

Because of a marginally stable average mode, the matrix A in (2) is not Hurwitz. The coordinate transformation (4) eliminates the average angle $\bar{\theta}$ from (2), thereby leading to (5) with Hurwitz $\bar{A}$. In the presence of stochastic disturbances, $\bar{\theta}(t)$ drifts in a random walk. Since $\bar{\theta}$ is not observable from the performance output z, z has a finite steady-state variance, determined by the square of the $\mathcal{H}_2$ norm of system (5).

B. Power spectral density and variance amplification

In what follows, we utilize an approach that offers additional and complementary insights to the conventional modal analysis. This approach is based on the input-output analysis, where the input d is the external disturbances and the z is performance output. In stochastically forced systems, input-output analysis amounts to the study of power spectral density and variance amplification. Our approach builds on the $\mathcal{H}_2$ paradigm [23], which analyzes and mitigates amplification of white stochastic disturbances.

We next provide a brief overview of the power spectral density and variance amplification analyses of linear dynamical systems. Let $H(j\omega)$ denote the frequency response of (5),

$$z(j\omega) \;=\; H(j\omega)\,d(j\omega).$$

The Hilbert-Schmidt norm determines the power spectral density of $H(j\omega)$,

$$\|H(j\omega)\|_{\mathrm{HS}}^2 \;=\; \mathrm{trace}\,(H(j\omega)\,H^*(j\omega)) \;=\; \sum \sigma_i^2(H(j\omega))$$

where σ_i's are the singular values of the matrix $H(j\omega)$. The $\mathcal{H}_2$ norm quantifies the steady-state variance (energy) of the output z of stochastically forced system (5). It is obtained by integrating the power spectral density over all

frequencies [23],

$$\|H\|_2^2 \;:=\; \lim_{t\to\infty} \mathbf{E}\left(z^T(t)\,z(t)\right) \;=\; \frac{1}{2\pi}\int_{-\infty}^{\infty} \|H(j\omega)\|_{\mathrm{HS}}^2\,\mathrm{d}\omega$$

where $\mathbf{E}$ is the expectation operator. Equivalently, the matrix solution X to the Lyapunov equation,

$$(\bar{A} \,-\, \bar{B}_2 F)\,X \;+\; X\,(\bar{A} \,-\, \bar{B}_2 F)^T \;=\; -\bar{B}_1\bar{B}_1^T$$

can be used to compute the $\mathcal{H}_2$ norm [23],

$$\begin{aligned} J(F) \;:=\; \|H\|_2^2 \;&=\; \mathrm{trace}\left(X\,(\bar{Q} \;+\; F^T R\,F)\right) \\ &=\; \mathrm{trace}\,(Z_1) \;+\; \mathrm{trace}\,(Z_2)\,. \end{aligned} \tag{6}$$

Here, X is the steady-state covariance matrix of the state ξ in (5), $X := \lim_{t\to\infty} \mathbf{E}\,(\xi(t)\,\xi^T(t))$, and the covariance matrices of the outputs z_1 and z_2 are determined by

$$\begin{aligned} Z_1 \;&:=\; \lim_{t\to\infty} \mathbf{E}\left(z_1(t)\,z_1^T(t)\right) \;=\; \bar{Q}^{1/2} X\,\bar{Q}^{1/2} \\ Z_2 \;&:=\; \lim_{t\to\infty} \mathbf{E}\left(z_2(t)\,z_2^T(t)\right) \;=\; R^{1/2} F\,X\,F^T R^{1/2}. \end{aligned}$$

Note that $\mathrm{trace}\,(Z_1)$ and $\mathrm{trace}\,(Z_2)$ quantify the system's kinetic and potential energy and the control effort, respectively. In particular, the eigenvalue decomposition of the matrix Z_1,

$$Z_1 \;=\; \sum \lambda_i\, y_i\, y_i^T$$

determines contribution of different *orthogonal* modes y_i to the kinetic and potential energy in statistical steady-state. The total energy is given by $\mathrm{trace}\,(Z_1)$, i.e., the sum of the eigenvalues λ_i of the covariance matrix Z_1. Each mode y_i contributes λ_i to the variance amplification and the spatial structure of the most energetic mode is determined by the principal eigenvector y_1 of the matrix Z_1.

III. Sparse and block-sparse optimal control

We study the problem of optimal signal selection and optimal design of wide-area controllers. We build on the framework developed in [10]–[13] which is aimed at finding a state feedback that simultaneously optimizes the closed-loop variance and induces a sparse control architecture.

A. Elementwise sparsity

As shown in Section II-B, the $\mathcal{H}_2$ norm of system (5) is determined by (6). While the $\mathcal{H}_2$ performance is expressed in terms of the feedback matrix F in the new set of coordinates, it is necessary to enhance sparsity of the feedback matrix K in the physical domain. This results in the regularized optimal control problem [13],

$$\begin{aligned} &\text{minimize} && J(F) \;+\; \gamma\, g(K) \\ &\text{subject to} && F\,T^T \;-\; K \;=\; 0. \end{aligned} \tag{7}$$

The regularization term in (7) is given by the weighted ℓ_1-norm of K, $g(K) := \sum_{i,j} W_{ij}|K_{ij}|$, which is an effective proxy for inducing elementwise sparsity [24]. The weights W_{ij}'s are updated iteratively using the solution to (7) from the previous iteration [24].

We solve the optimal control problem (7) for different values of the positive regularization parameter γ via the alternating direction method of multipliers; see [12], [13] for algorithmic details. This allows us to identify a parameterized family of distributed control architectures that strikes a balance between performance and sparsity requirements.

B. Block sparsity

In power systems, only rotor angle differences enter into the dynamics and information about absolute angles is not available. It is thus advantageous to treat rotor angles separately from the remaining states in the control design. We partition K conformably with partition of the state vector x,

$$K \;=\; \left[\begin{array}{cc} K_\theta & K_r \end{array}\right]$$

where K_θ and K_r are the feedback gains acting on the rotor angles and the remaining states, respectively.

While our approach is general, in the sequel we restrict our presentation to Power System Stabilizers (PSSs) as actuators. For PSSs the control action is usually formed in a fully-decentralized fashion using local measurements of frequencies and power injections. We represent r as $\left[\begin{array}{ccc} r_1^T & \cdots & r_N^T \end{array}\right]^T$, where r_i is the vector of states of the controlled generator i (modulo angles). If K_r is partitioned conformably with the partition of the vector r, then the block-diagonal elements of K_r provide a means for retuning the local control action. Since r_i is readily available to the controller of generator i, in what follows we do not introduce sparsity-promoting penalty on the block-diagonal elements of K_r. In this paper, group penalties are imposed on the states of all other generators in K_r, see [20] for additional options and details regarding block-sparsity setup.

IV. Case study: NETS-NYPS Test System

The New England Test System (NETS)−New York Power System (NYPS) example consists of 16 machines, 68 buses and 5 areas; see Fig. 1. All the generators have fast static excitation system, while generators $1-12$ are also equipped with Power System Stabilizers (PSSs). A detailed description of the model can be found in [18], [19].

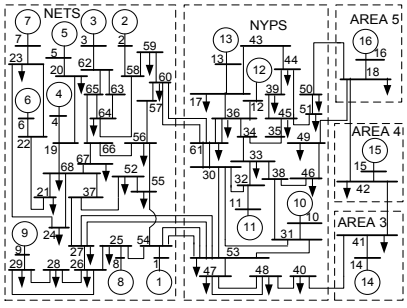

Fig. 1: Schematic diagram of NETS-NYPS test system.

The uncontrolled open-loop system is unstable, and PSSs are used for stabilization and to suppress local oscillations. For the subsequent analysis and the wide-area control design, we assume that the PSS inputs are embedded in the open-loop matrix $A \in \mathbb{R}^{147\times 147}$ in (2). The transfer function of

TABLE I: Poorly-damped modes of A with PSSs

mode no.	eigenvalue pair	damping ratio	freq. [Hz]	coherent groups
1	$-0.2634 \pm \mathrm{j}\, 6.9464$	0.0379	1.1061	1,8,9 vs.2,3 vs.4-7
2	$-0.3268 \pm \mathrm{j}\, 7.8543$	0.0416	1.2510	2,3,13 vs. 10-12
3	$-0.3347 \pm \mathrm{j}\, 7.0581$	0.0474	1.1252	2,3 vs. 4-7 vs. 9
4	$-0.4113 \pm \mathrm{j}\, 8.3783$	0.0490	1.3353	10,11 vs. 12

the local PSS controller on the ith generator is given by

$$u_i(s) \;=\; k_i \cdot \frac{T_{w,i}s}{1+T_{w,i}s} \cdot \frac{1+T_{n1,i}s}{1+T_{d1,i}s} \cdot \frac{1+T_{n2,i}s}{1+T_{d2,i}s} \cdot \dot{\theta}_i(s)$$

with $T_{w,i} = 5$, $T_{n1,i} = T_{n2,i} = 0.08$, $T_{d1,i} = T_{d2,i} = 0.02$, $k_i = 4$ for $i \in \{1, \cdots, 12\}$. This set of PSS control gains stabilizes the unstable open-loop system.

A. Analysis of the open-loop system with PSSs

Despite the action of the local PSS controllers, modal and participation factor analyses still reveal the presence of four poorly-damped modes; see Table I. The dominant inter-area modes have damping ratios as low as 3.79% and 4.16%. Therefore, the local PSS controllers need to be complemented by supplementary wide-area controllers to improve the damping of the inter-area oscillations.

Figure 2 illustrates the power spectral density of the open-loop system. The largest peak occurs at $\omega_1 = 6.9464$ rad/s ($f_1 = \omega_1/2\pi = 1.1061$ Hz) and it corresponds to mode 1 in Table I. Note that the other two resonant peaks are local modes that have reasonable damping ratios greater than 5%.

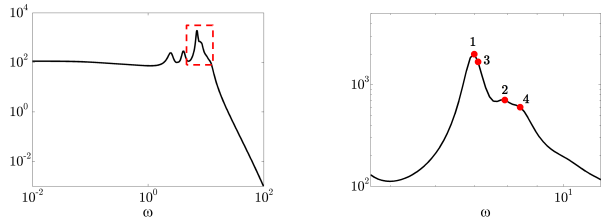

(a) (b)

Fig. 2: (a) Power spectral density of the open-loop system; (b) zoomed version of the red square shown in (a). Red dots denote poorly-damped modes from Table I.

The contribution of each generator to the steady-state variance is shown in Fig. 3. The diagonal elements of Z_1 contain information about mean-square deviation from angle average and variance amplification of frequencies of the individual generators. From Fig. 3, we see that the largest contribution to the variance amplification arises from the misalignment of angles and frequencies of generators 9.

Similar observations can be made from Fig. 4. In Fig. 4a, we observe two dominant eigenvalues of Z_1. We also show the spatial structure of these two principal eigenvectors (modes) of Z_1, which contain about 30% of the total variance. Although the angle and frequency fluctuations in experiments and nonlinear simulations are expected to be more complex than the structures presented in Fig. 4, the spatial profiles identified here are likely to play significant role in amplification of disturbances in power systems.

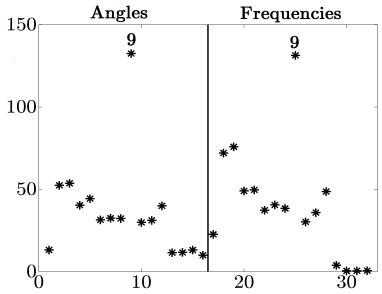

Fig. 3: Diagonal elements of the open-loop covariance matrix Z_1 determine contribution of each generator to the variance amplification.

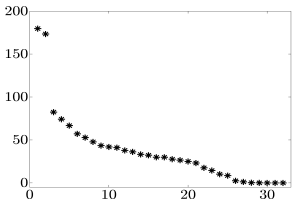

(a) Eigenvalues of Z_1

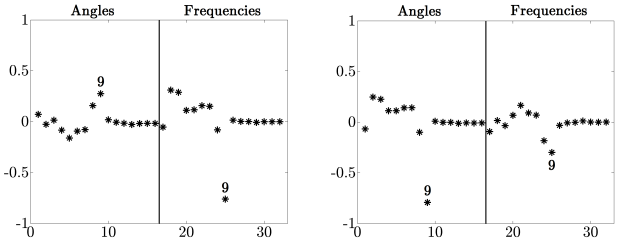

(b) $\lambda_1(Z_1)$ (c) $\lambda_2(Z_1)$

Fig. 4: (a) Eigenvalues; and (b),(c) eigenvectors corresponding to the three largest eigenvalues λ_i of the open-loop output covariance matrix Z_1.

B. Sparsity-promoting optimal wide-area control

1) Elementwise sparsity: We first consider an optimal sparse controller whose structure is identified using the solution to (7). Sparsity patterns of the feedback matrix $K \in \mathbb{R}^{12\times 147}$ for different values of γ are illustrated in Fig. 5. The blue dots denote information coming from the generators on which the particular controller acts, and the red dots identify information that needs to be communicated from other generators. For $\gamma = 0.5574$ and $\gamma = 0.8490$, the identified wide-area control architecture indicate that the controller of generator 1 needs to have access to the difference between its angle and the angle of generator 9.

When γ is increased to 3, we obtain a fully-decentralized controller. Compared to the optimal centralized controller,

our fully-decentralized controller degrades the closed-loop performance by about 13.09%; see Fig. 6. This fully-decentralized controller can be embedded into the local generator excitation system by directly feeding the local measurements to the automatic voltage regulator, thereby effectively retuning the PSS controller.

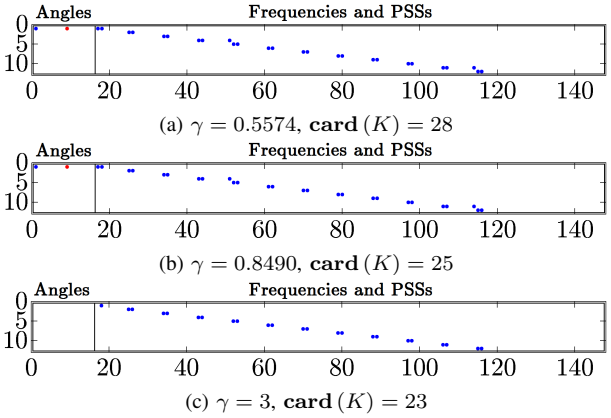

(a) $\gamma = 0.5574$, $\mathbf{card}\,(K) = 28$

(b) $\gamma = 0.8490$, $\mathbf{card}\,(K) = 25$

(c) $\gamma = 3$, $\mathbf{card}\,(K) = 23$

Fig. 5: Sparsity patterns of K resulting from (7).

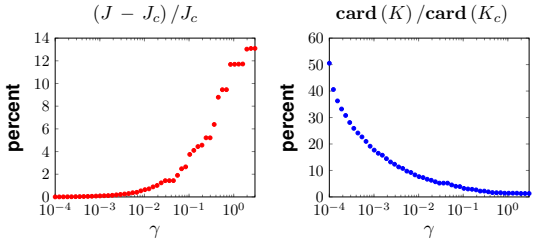

Fig. 6: Performance vs sparsity comparison of sparse K and the optimal centralized controller K_c for 50 logarithmically-spaced points $\gamma \in [\,10^{-4}\,,\,3\,]$.

2) Block sparsity: Three identified block-sparsity patterns of the feedback matrix are shown in Fig. 7. When $\gamma = 0.1$, we obtain a fully-decentralized controller structure. The group penalty yields block-diagonal feedback gains that act on the remaining states of generators 1-12. Since no information exchange with generators $13-16$ is required, this part of K is implemented in a fully-decentralized fashion.

Compared to the optimal centralized controller, a fully-decentralized controller with structure shown in Fig. 7c compromises performance by only 2.56% for system of such large dimension; see Fig. 8. We recall that the fully-decentralized controller with structure shown in Fig. 5c degrades performance by 13.09%; cf. Fig. 6. Since the block-sparse controller has more degrees of freedom than the elementwise sparse controller, performance improvement does not come as a surprise. We finally note that the jumps in the number of non-zero elements in Fig. 8 are caused by elimination of the entire off-diagonal rows of K_r.

C. Comparison of open- and closed-loop systems

We next compare performance of the open-loop system and the closed-loop systems with optimal centralized and

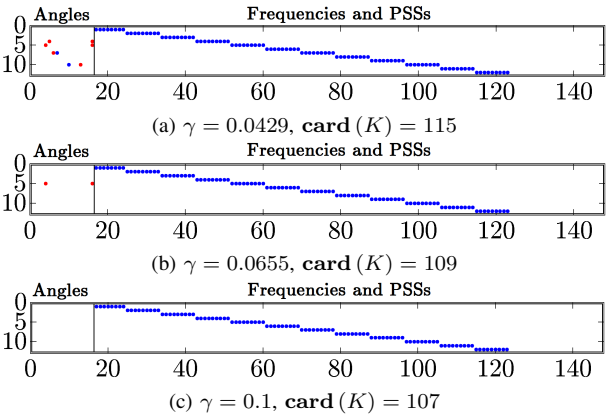

(a) $\gamma = 0.0429$, $\mathbf{card}\,(K) = 115$

(b) $\gamma = 0.0655$, $\mathbf{card}\,(K) = 109$

(c) $\gamma = 0.1$, $\mathbf{card}\,(K) = 107$

Fig. 7: Sparsity patterns of K.

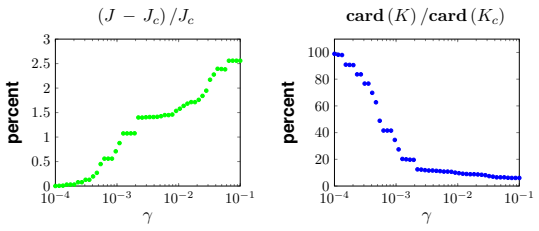

Fig. 8: Performance vs sparsity comparison of block-sparse K and the optimal centralized controller K_c for 50 logarithmically-spaced points $\gamma \in [\,10^{-4}\,,\,0.1\,]$.

fully-decentralized sparse and block-sparse controllers. The structures of these fully-decentralized controllers are shown in Fig. 5c and Fig. 7c, respectively.

Figure 9 provides a comparison between the power spectral densities of four cases. All three controllers successfully suppress resonant peaks associated with the poorly-damped modes in Table I and significantly improve performance. We also note that the fully-decentralized block-sparse controllers perform almost as well as the optimal centralized controller for high frequencies; for low frequencies, we observe minor performance degradation in the variance amplification.

D. Robustness analysis

We then examine robustness to the operating point changes of both open- and closed-loop systems. Random load pertur-

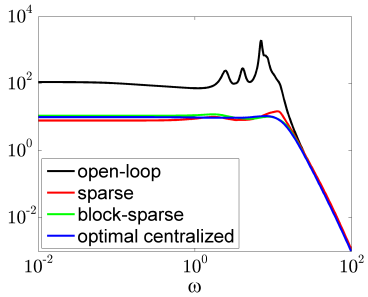

Fig. 9: Power spectral density comparison.

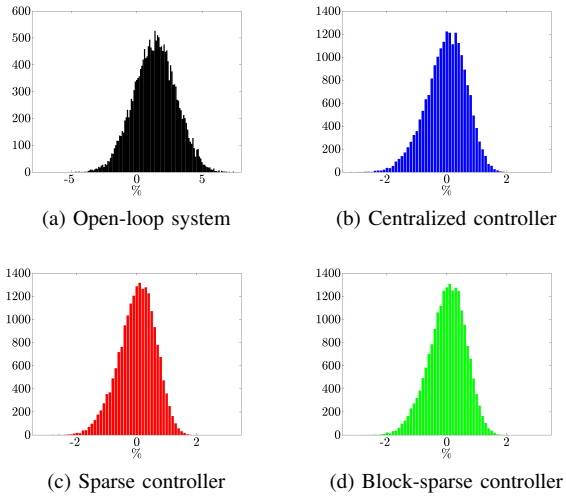

(a) Open-loop system (b) Centralized controller

(c) Sparse controller (d) Block-sparse controller

Fig. 10: Performance histograms of open- and closed-loop linearized systems (with nominal controllers) for $20,000$ uniformly distributed operating points.

bations are used to modify the operating point of the nonlinear system. The loads are altered via uniformly distributed perturbations that are within $\pm 20\%$ of the nominal loads. The performance of the *nominal* centralized and decentralized controllers on the *perturbed linearized model* is evaluated by examining the closed-loop $\mathcal{H}_2$ norm.

Figure 10 shows the distribution of performance change for $20,000$ operating points around the original equilibria. We observe bell-shaped distributions with symmetric and narrow spread around the nominal performance. In spite of significant changes in the operating points, both centralized and fully-decentralized controllers are within 2% of the nominal performance. In contrast, same perturbations can degrade performance of the open-loop system by as much as 6%. Thus, our decentralized controllers also reduce the sensitivity and improve the robustness with respect to setpoint changes.

V. Concluding remarks

We have analyzed inter-area oscillations in power systems by studying their power spectral densities and output covariances. We have also designed sparse and block-sparse feedback controllers that use relative angle measurements to achieve a balance between system performance and controller architecture. By placing increasing weight on the sparsity-promoting term we obtain fully-decentralized feedback gains. Performance comparisons of open- and closed-loop systems allowed us to understand the effect of the control design approach both in terms of system performance and with regards to the resulting control architecture. For the NETS-NYPS test system we have successfully tested our analysis and control design algorithms. We have also provided a systematic method for optimal retuning of fully-decentralized excitation controllers that achieves comparable performance to the optimal centralized controller.

References

[1] F. Alvarado, C. DeMarco, I. Dobson, P. Sauer, S. Greene, H. Engdahl, and J. Zhang, "Avoiding and suppressing oscillations," *PSERC Project Final Report*, 1999.

[2] M. Klein, G. J. Rogers, S. Moorty, and P. Kundur, "Analytical investigation of factors influencing power system stabilizers performance," *IEEE Transactions on Energy Conversion*, vol. 7, no. 3, pp. 382–390, 1992.

[3] T. Othman, J. J. Sanchez-Gasca, M. A. Kale, and J. H. Chow, "On the design of robust power system stabilizers," in *Proceedings of the 28th IEEE Conference on Decision and Control*, 1989, pp. 1853–1857.

[4] J. A. Taylor and L. Scardovi, "Decentralized control of DC-segmented power systems," in *Proceedings of the 52th Annual Allerton Conference*, 2014, pp. 1046–1050.

[5] J. Xiao, F. Wen, C. Y. Chung, and K. P. Wong, "Wide-area protection and its applications–a bibliographical survey," in *IEEE PES Power Systems Conference and Exposition*, 2006, pp. 1388–1397.

[6] Y. Zhang and A. Bose, "Design of wide-area damping controllers for interarea oscillations," *IEEE Trans. Power Syst.*, vol. 23, no. 3, pp. 1136–1143, 2008.

[7] L. P. Kunjumuhammed, R. Singh, and B. C. Pal, "Robust signal selection for damping of inter-area oscillations," *IET Generation, Transmission & Distribution*, vol. 6, no. 5, pp. 404–416, 2012.

[8] B. Bamieh, M. R. Jovanović, P. Mitra, and S. Patterson, "Coherence in large-scale networks: dimension dependent limitations of local feedback," *IEEE Trans. Automat. Control*, vol. 57, no. 9, pp. 2235–2249, 2012.

[9] M. Fardad, F. Lin, and M. R. Jovanović, "Design of optimal sparse interconnection graphs for synchronization of oscillator networks," *IEEE Trans. Automat. Control*, vol. 59, no. 9, pp. 2457–2462, 2014.

[10] M. Fardad, F. Lin, and M. R. Jovanović, "Sparsity-promoting optimal control for a class of distributed systems," in *Proceedings of the 2011 American Control Conference*, 2011, pp. 2050–2055.

[11] F. Lin, M. Fardad, and M. R. Jovanović, "Sparse feedback synthesis via the alternating direction method of multipliers," in *Proceedings of the 2012 American Control Conference*, 2012, pp. 4765–4770.

[12] F. Lin, M. Fardad, and M. R. Jovanović, "Design of optimal sparse feedback gains via the alternating direction method of multipliers," *IEEE Trans. Automat. Control*, vol. 58, no. 9, pp. 2426–2431, 2013.

[13] X. Wu and M. R. Jovanović, "Sparsity-promoting optimal control of consensus and synchronization networks," in *Proceedings of the 2014 American Control Conference*, 2014, pp. 2948–2953.

[14] F. Dörfler, M. R. Jovanović, M. Chertkov, and F. Bullo, "Sparse and optimal wide-area damping control in power networks," in *Proceedings of the 2013 American Control Conference*, 2013, pp. 4295–4300.

[15] F. Dörfler, M. R. Jovanović, M. Chertkov, and F. Bullo, "Sparsity-promoting optimal wide-area control of power networks," *IEEE Trans. Power Syst.*, vol. 29, no. 5, pp. 2281–2291, 2014.

[16] S. Schuler, U. Münz, and F. Allgöwer, "Decentralized state feedback control for interconnected systems with application to power systems," *Journal of Process Control*, vol. 24, no. 2, pp. 379–388, 2014.

[17] X. Wu, F. Dörfler, and M. R. Jovanović, "Analysis and design trade-offs for power network inter-area oscillations," in *Proceedings of the 21st International Symposium on Mathematical Theory of Network and Systems*, Groningen, The Netherlands, 2014, pp. 657–663.

[18] B. Pal and B. Chaudhuri, *Robust control in power systems*. Springer, 2005.

[19] A. Singh and B. Pal, "Decentralized dynamic state estimation in power systems using unscented transformation," *IEEE Trans. Power Syst.*, vol. 29, no. 2, pp. 794–804, 2014.

[20] X. Wu, F. Dörfler, and M. R. Jovanović, "Input-output analysis and decentralized optimal control of inter-area oscillations in power systems," *IEEE Trans. Power Syst.*, 2015, doi:10.1109/TPWRS.2015.2451592; also arXiv:1502.03221.

[21] P. Kundur, *Power system stability and control*. McGraw-Hill, 1994.

[22] D. Romeres, F. Dörfler, and F. Bullo, "Novel results on slow coherency in consensus and power networks," in *Proceedings of the 12th European Control Conference*, 2013, pp. 742–747.

[23] G. E. Dullerud and F. Paganini, *A course in robust control theory*. Springer, 2000.

[24] E. J. Candès, M. B. Wakin, and S. P. Boyd, "Enhancing sparsity by reweighted ℓ_1 minimization," *J. Fourier Anal. Appl*, vol. 14, pp. 877–905, 2008.